Chapter-5

Study of $SrTiO_3$ Based Perovskite Material for developing superior oxide-ion electrolyte

5.1 Introduction

High-temperature ferroelectric materials are of technological interest. With increasing environmental concerns, efforts are being made to search for more environmentally friendly lead-free ferroelectric material for Oxide-ion conductors in SOFCs. PZT based materials have a superior dielectric constant and ferroelectricity only due to the small size of Ti cation present in the octahedral structure. So if we create oxide-ion vacancy in higher dielectric samples, we can get a superior conductivity. $SrTiO_3$ is also well known for its incipient ferroelectric behaviour;[1-2] we have chosen it as a host material to develop the oxide-ion conductor. Similar to the previous one, this chapter deals with ionic conductivities of simultaneously substituted K & Ga doped $SrTiO_3$.

In most perovskite and fluorite-based materials studied, oxide-ion conductivity improves at higher temperatures in the mobile oxide-ion vacancy conduction model[3-9]. Similar to $BaZrO_3$[9], we have done simultaneous doping of smaller Ga on the Ti site and K on the Sr site to create a higher concentration of oxide-ion vacancies to realize superior conductivities.

5.2 Material synthesis and characterization

$Sr_{1-x}K_xTi_{1-y}Ga_yO_{3-\delta}$ samples were synthesized by solid-state ceramic route by mixing stoichiometric amounts of $SrCO_3$, K_2CO_3, TiO_2 and Ga_2O_3, subsequently heating them for 15 hours at 1050°C. For obtaining the single-phase material, multiple heating cycles were carried out. Samples were heated multiple times at 1050°C for 15 hours with the intermediate grinding of the sample. For conductivity measurement, the powder was made into pellets of 10 mm diameter and ~0.2-0.25cm thickness by pressing it to 6-7 ton weight on a hydraulic press. These pellets were fired at 1150°C for 12 hours for densification. The pellet density was measured using the Archimedes method, and it was found to be ~97% of the theoretical density of the material.

The phase formation study was carried out through Rigaku Miniflex desktop X-ray Diffractometer (XRD) with Cu-Kα radiation (λ = 1.54 Å) in the range 2θ ~ 10 - 90° with a step size of 0.02°. The structures were refined by the Rietveld refinement method using FULLPROF suite software package and cubic perovskite $SrTiO_3$ (space group: Pm-3m) as model structure. The microstructures of the sintered samples were investigated by using scanning electron microscopy (EVO - Scanning Electron Microscope MA15/18). The average grain size was calculated using the linear intercept method. The composition of the compounds was examined by Energy dispersive X-ray (EDX) spectroscopy with a probe attached to the SEM instrument.

The total conductivity measurements of all the samples were carried out using an impedance analyzer, AUTOLAB, Netherlands, from 1MHz to 1 Hz in the temperature range 300 °C to 650°C in different atmospheres. Pt was used as current collector on both 'opposite' sides of the pellets for conductivity measurements. The total conductivity of samples is determined from the intercepts of the semicircle on the real axis by using the following relationship:

$$\sigma = l/RA \ Scm^{-1} \qquad \text{eq(5.1).}$$

where l/A is the geometrical factor, l is the thickness, A is the area of the sample, and R is the total resistance which is indicated by the intercept of the semicircle on the real axis. The sintered pellets were coated with silver paste and cured at 500°C for 30 minutes. All measurements were taken during the cooling cycle from 650°C to 100°C.

5.3 Crystal Structure Study

Up to 25% of K at Sr site and 25% Ga at Ti site simultaneously substituted were in $SrTiO_3$ lattice. The crystal structure and phase purity of the material was studied by powder XRD. Powder XRD pattern of $Sr_{0.9}K_{0.1}Ti_{0.9}Ga_{0.1}O_{2.9}$ (SK10G10), $Sr_{0.85}K_{0.15}Ti_{0.85}Ga_{0.15}O_{2.85}$ (SK15G15), $Sr_{0.8}K_{0.2}Ti_{0.8}Ga_{0.2}O_{2.8}$ (SK20G20), $Sr_{0.75}K_{0.25}Ti_{0.75}Ga_{0.25}O_{2.75}$ (SK25G25) are shown Figure 5.2 (b-d) respectively. All the peaks were identified as $SrTiO_3$ structures (JCPDS No: 35-074). No impurity peaks were identified for any $SrCO_3$, K_2CO_3 or Ga_2O_3 phases. There is a systematic increase in the lattice parameter of $Sr_{1-x}K_xTi_{1-y}Ga_yO_{3-x}$ with increasing K and Ga content which can be concluded as 2θ shifted to a lower value with an increase in doping concentration.

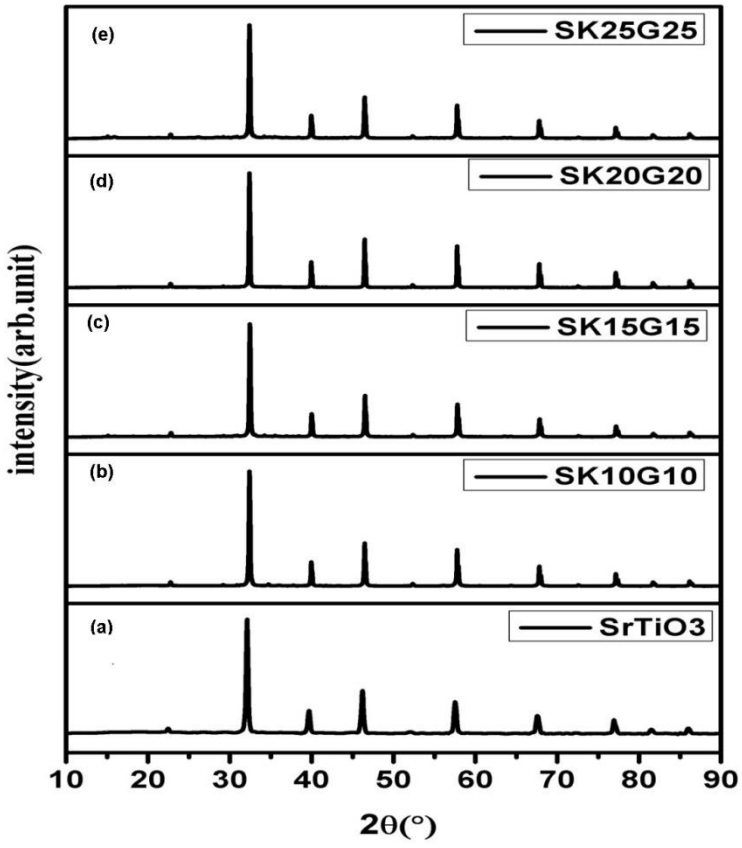

Figure 5.1 Powder XRD pattern (a) $SrTiO_3$ (b)$Sr_{0.9}K_{0.1}Ti_{0.9}Ga_{0.1}O_{2.9}$ (SK10G10) (c) $Sr_{0.85}K_{0.15}Ti_{0.85}Ga_{0.15}O_{2.85}$ (SK15G15) (d) $Sr_{0.8}K_{0.2}Ti_{0.8}Ga_{0.2}O_{2.8}$ (SK20G20) (e) $Sr_{0.75}K_{0.25}Ti_{0.75}Ga_{0.25}O_{2.75}$ (SK25G25)

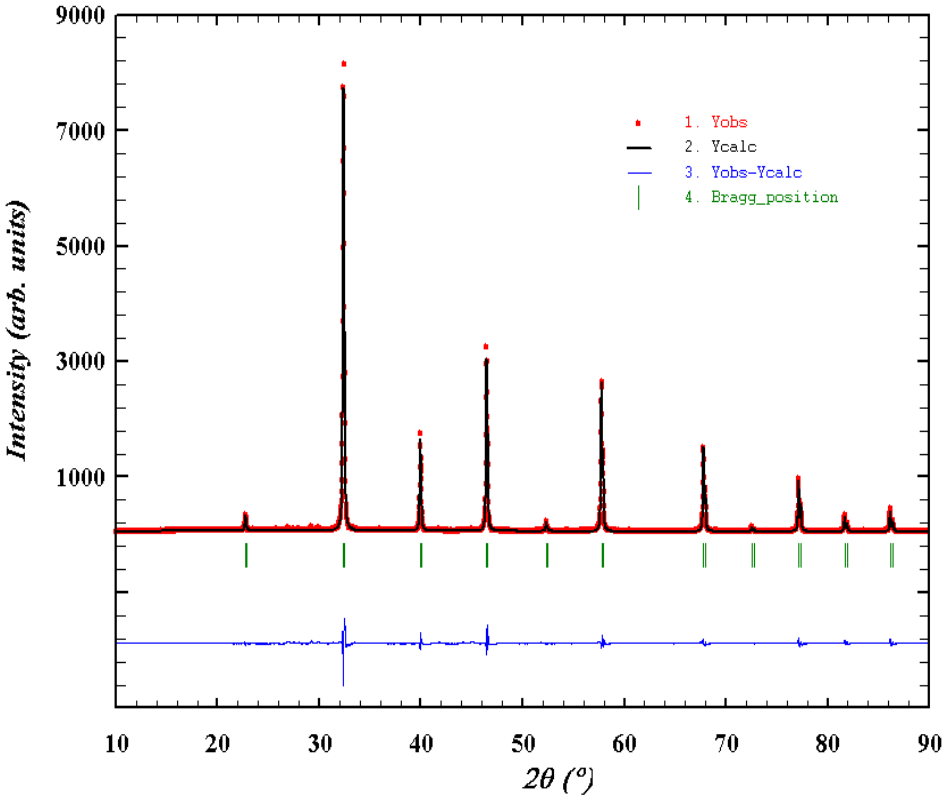

Figure 5.2. (a) Rietveld refined powder XRD profile of $Sr_{0.9}K_{0.1}Ti_{0.9}Ga_{0.1}O_{2.9}$

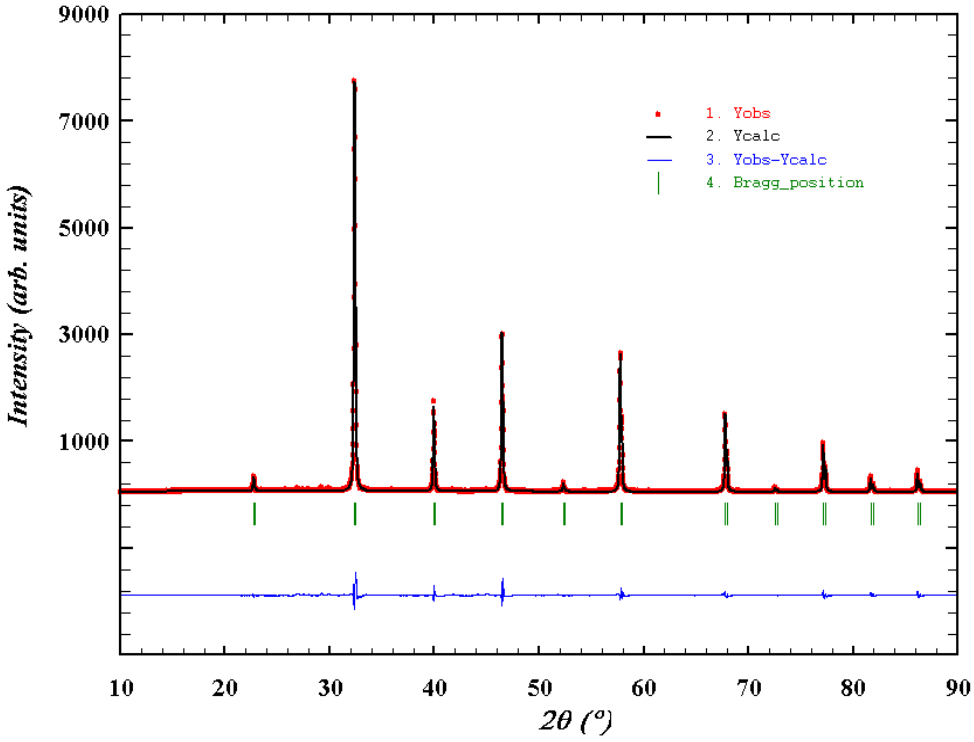

Figure 5.2. (b) Rietveld refined powder XRD profile of $Sr_{0.8}K_{0.2}Ti_{0.8}Ga_{0.2}O_{2.8}$

Crystal structures of K and Ga substituted $SrTiO_3$ were refined using the Rietveld method. For this purpose, XRD of preheated samples was recorded at a slow scan rate 1^o per minute with 0.01^o step size. Figure 5.2- shows the Rietveld refined XRD profile of (a) $Sr_{0.9}K_{0.1}Ti_{0.9}Ga_{0.1}O_{2.9}$, (b) $Sr_{0.8}K_{0.2}Ti_{0.8}Ga_{0.2}O_{2.8}$ We can see that fitted profile matched well with the observed XRD pattern. The structural parameters obtained from the Reitveld refinement of powder XRD pattern are shown in Table 5.1. The lattice parameter of $SrTiO_3$ was found to be 3.9452Å, and for $Sr_{0.75}K_{0.25}Ti_{0.75}Ga_{0.25}O_{2.75}$, it was found to be 3.9492Å. The lattice parameter of $Sr_{0.8}K_{0.2}Ti_{0.8}Ga_{0.2}O_{2.8}$ was also found at 3.9484Å (higher than the lattice parameter of undoped $SrTiO_3$).

Table 5.1: Structural parameter of K and Ga doped $SrTiO_3$

Compound	**Lattice parameter(Å) (a=b=c)**	χ^2	R_f	R_{Bragg}
$SrTiO_3$	*3.9452(2)*	0.67	1.12	2.98
$Sr_{0.9}K_{0.1}Ti_{0.9}Ga_{0.1}O_{2.9}$	3.9461(3)	2.15	5.34	3.27
$Sr_{0.85}K_{0.15}Ti_{0.85}Ga_{0.15}O_{2.85}$	3.9476(1)	1.28	4.32	2.31
$Sr_{0.8}K_{0.2}Ti_{0.8}Ga_{0.2}O_{2.8}$	3.9484(2)	0.52	2.38	2.22
$Sr_{0.75}K_{0.25}Ti_{0.75}Ga_{0.25}O_{2.75}$	3.9492(2)	3.03	5.17	4.76

The substitution of K^+ and Ga^{3+} on Sr & Ti sites, respectively, in $SrTiO_3$ lattice shows a slight increase in the lattice parameter with an increase in doping. Point to be noted that K^+ and Ga^{3+} ion is slightly greater than Sr^{2+} ion in 12 coordination & Ti^{4+} ion in six coordination, respectively.[10] Thus, due to the rigid nature of the octahedral network in the 3-d structure of the perovskite lattice and compensation due to different size cations (K^+ and Ga^{3+} ions substitution in the $SrTiO_3$ lattice) results, only a slight change in the lattice parameter of doped $SrTiO_3$ based perovskites.

5.4 Thermal Study

TGA studies were carried out to know the weight loss due to water/moisture absorption and desorption on the materials and the associated phase changes that may occur due to this. The as preheated sample of $Sr_{0.8}K_{0.2}Ti_{0.8}Ga_{0.2}O_{2.8}$ was thermal analyzed in Thermogravimetric and (TGA) analysis at a constant heating rate of 10 ^oC/minute in the temperature range of 30^oC – 900^oC. Figure 5.3 demonstrates the TGA curve of the pure $Sr_{0.8}K_{0.2}Ti_{0.8}Ga_{0.2}O_{2.8}$ sample. The first stage of weight loss that occurs up to 80°C is due to the loss of the adsorbed moisture and structural water present in the sample after exposure to the atmosphere. The second stage of weight loss, around 320-480°C, is due to removing absorbed or strongly bonded carbonaceous species present in the materials and is attributed to the final phase formation. TGA study confirms the relatively low hygroscopic nature (1.1% weight loss up to 400^oC and a total 1.4% weight loss up to 500^oC) of the materials and the absence of absorbed moisture in the sample above 400^oC. Thus the TGA studies confirm the structural stability of the material in the temperature range of 30^oC-900^oC.

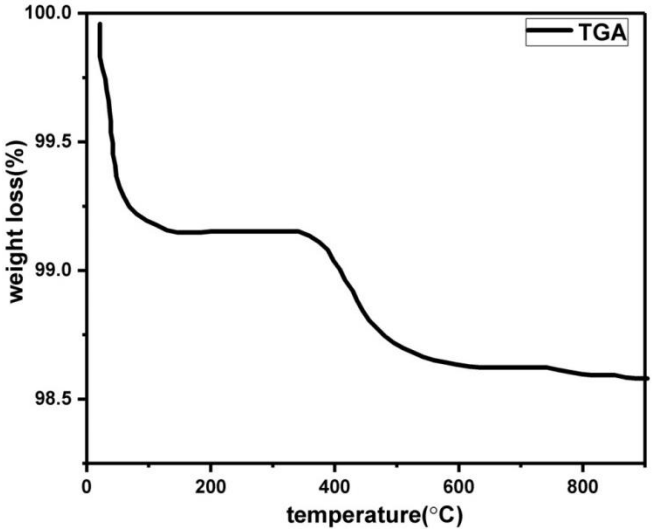

Figure 5.3 Thermogravimetric analysis (TGA) of $Sr_{0.8}K_{0.2}Ti_{0.8}Ga_{0.2}O_{2.8}$

5.5 SEM Study

SEM micrographs of $Sr_{0.8}K_{0.2}Ti_{0.8}Ga_{0.2}O_{2.8}$ (powder, cross-section of the pellet utilized for conductivity measurement) are given in Figure 5.4(a-c). The SEM study reveals that the powder sample contains dense grains of 3–8μm in size. No colour contrast was observed in the SEM images suggesting a single phase of the materials forming the grains. Figure 5.4(b) shows the images of the cross-section of the pellet. The microstructure of the pellets shows the good density of the pellet, and the grains are in good contact with each other due to crystal growth during sintering. The EDX study with the probe attached to the SEM instrument (micrograph shown in Figure 5.4(c)) also confirms that the composition of the materials is close to the nominal composition taken for the synthesis of the material.

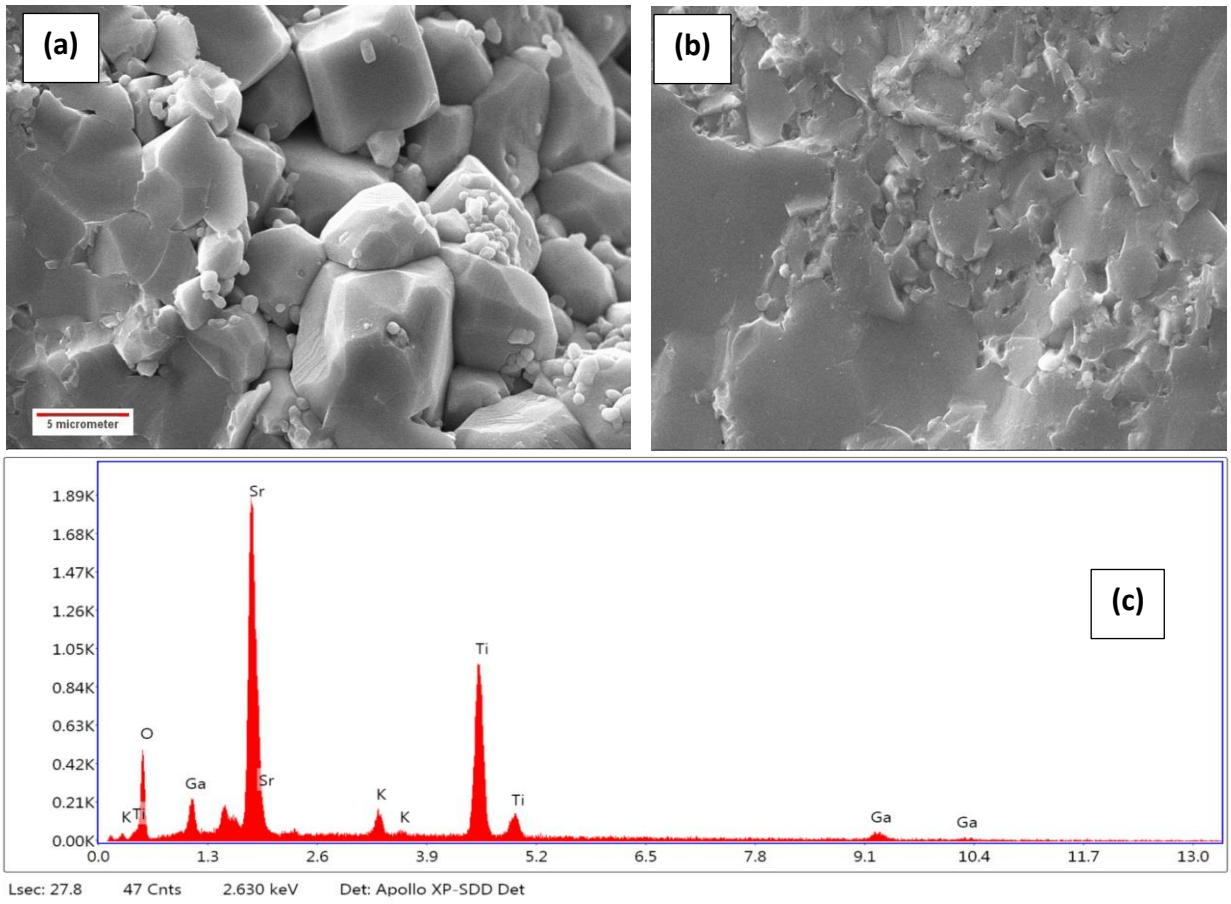

Figure 5.4. SEM image $Sr_{0.8}K_{0.2}Ti_{0.8}Ga_{0.2}O_{2.8}$ (a) Powder (b) pellet (c) EDX image of pallet

Thus XRD, SEM with EDX study confirms that K^+ and Ga^{3+} ion are substituted in $SrTiO_3$ lattice respectively at Sr^{2+} and Ti^{4+} sites. Considering the intrinsic stoichiometric defects, the substitution of K^+ at the Sr^{2+} site and substitution of Ga^{3+} and Ti^{4+} will create oxygen vacancy formation and the defect formation equation using Kröger–Vink notation can be represented as:

$$K_{Sr}^{'} + Ga_{Ti}^{'} \leftrightarrow V_o^{\cdot\cdot} \qquad \text{eq (5.2)}$$

5.6 Impedance Study

Oxide-ion conductivity or total ionic conductivity studies of the materials were carried out using an impedance spectrometer at various temperatures in different environments. Figure 5.5 show the oxide-ion conductivity for different composition of K and Ga substituted $SrTiO_3$ i.e. (i) $Sr_{0.9}K_{0.1}Ti_{0.9}Ga_{0.1}O_{2.9}$ (ii) $Sr_{0.85}K_{0.15}Ti_{0.85}Ga_{0.15}O_{2.85}$ (iii) $Sr_{0.8}K_{0.2}Ti_{0.8}Ga_{0.2}O_{2.8}$ (iv) $Sr_{0.75}K_{0.25}Ti_{0.75}Ga_{0.25}O_{2.75}$. The conductivity was found continuously increase with increasing temperature for all the compositions. The best oxide-ion conductivity of this series was observed for the composition $Sr_{0.8}K_{0.2}Ti_{0.8}Ga_{0.2}O_{2.8,}$ and at 650°C, the measured oxide-ion conductivity was ~10^{-2} S.cm^{-1} for the material. A sudden increase in oxide-ion conductivity was observed over 400^{o}C of all the samples except $Sr_{0.8}K_{0.2}Zr_{0.8}Ti_{0.2}O_{2.8,}$ in which this sudden increase can be seen at 350 ^{o}C itself. We also calculated the activation energy of conduction using the Arrhenius equation below 400^{o}C and above 400^{o}C. The change in conductivity and activation energy is very similar for the reported perovskite oxide-ion conductors such as $La_{1-x}Sr_xGa_{1-y}Mg_yO_{3-(x+y)/2}$[11-14], $Na_{0.5}Bi_{0.5}TiO_3$[15-16] & $Ba_{0.8}K_{0.2}Zr_{0.8}Ga_{0.2}O_{2.8.}$[9] We have seen a similar trend of conductivity as BKZGO up to 450^{o}C and then up to 600^{o}C; it was observed a dramatic change in conductivity. We believe in the K and Ga doped $SrTiO_3$ based system also the same mechanism of mobile vacancy percolation is also occurring. The conductivity presented here for the $Sr_{0.8}K_{0.2}Ti_{0.8}Ga_{0.2}O_{2.8}$ sample is better or equivalent to the conductivity obtained for YSZ (yttria-stabilized zirconia); a well-known ceramic oxide-ion electrolyte employed solid oxide fuel cells. Table 5.2 presents the conductivities of different compounds commonly used as oxide-ion electrolytes for SOFCs.

Table 5.2 O^{2-} conductivity (σ) of $Sr_{1-x}K_xTa_{1-y}Ga_yO_{3-\delta}$ at different temperatures

	Conductivity ($S.cm^{-1}$)			
Compound	***650°C***	**600°C**	**550°C**	**500°C**
$Sr_{0.9}K_{0.1}Ti_{0.9}Ga_{0.1}O_{2.9}$	$2.8x10^{-4}$	$1.9x10^{-4}$	$0.5x10^{-4}$	$9.8x10^{-5}$
$Sr_{0.85}K_{0.15}Ti_{0.85}Ga_{0.15}O_{2.85}$	$3.1x10^{-3}$	$4.5x10^{-4}$	$2.2x10^{-4}$	$1.6x10^{-4}$
$Sr_{0.8}K_{0.2}Ti_{0.8}Ga_{0.2}O_{2.8}$	**$1.5x10^{-2}$**	**$8.6x10^{-3}$**	**$1.8x10^{-3}$**	**$1.2x10^{-3}$**
$Sr_{0.75}K_{0.25}Ti_{0.75}Ga_{0.25}O_{2.75}$	$2.8x10^{-3}$	$5.5x10^{-3}$	$1.1x10^{-3}$	$1.9x10^{-4}$
$Ba_{0.8}K_{0.2}Zr_{0.8}Ga_{0.2}O_{2.8}$ (Ref. 9)	$2.1x10^{-2}$	$8.8x10^{-3}$	$3.3x10^{-3}$	$1.6x10^{-3}$
$KTa_{0.4}Ti_{0.3}Ge_{0.3}O_{2.7}$ (Ref. 8)	$5.2x10^{-2}$	$3.1x10^{-2}$	$9.8x10^{-3}$	$8.5x10^{-3}$
$Na_{0.5}Bi_{0.49}Ti_{0.98}Mg_{0.02}O_{2.965}$ (Ref. 5)		$5.6x10^{-3}$	$5.4x10^{-3}$	$3.5x10^{-3}$
$Zr_{0.92}Y_{0.08}O_{1.96}$ (Ref. 5)		$4.4x10^{-3}$	$2.3x10^{-3}$	$1x10^{-3}$
$Ce_{0.9}Gd_{0.1}O_{1.95}$ (Ref. 5)		$2.3x10^{-2}$	$1.2x10^{-2}$	$5.5x10^{-3}$
$La_{0.9}Sr_{0.1}Ga_{0.9}Mg_{0.1}O_{2.9}$ (Ref. 5)		$2.5x10^{-2}$	$1.5x10^{-2}$	$5.5x10^{-3}$

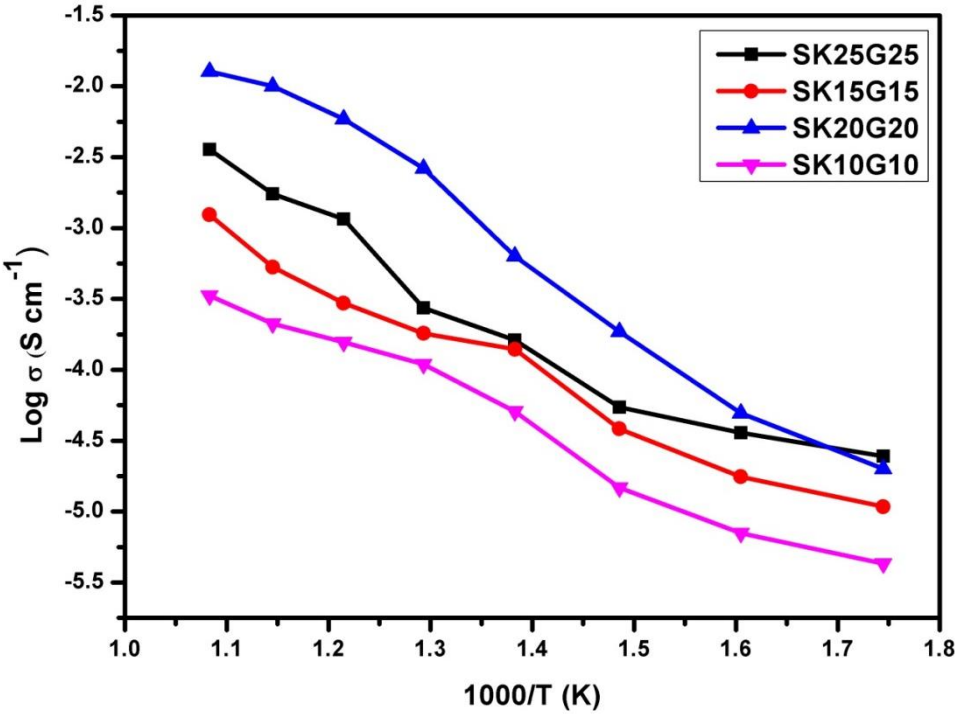

Figure 5.5 Arrhenius plots of various compositions $Sr_{1-x}K_xTi_{1-y}Ga_yO_{3-\delta}$

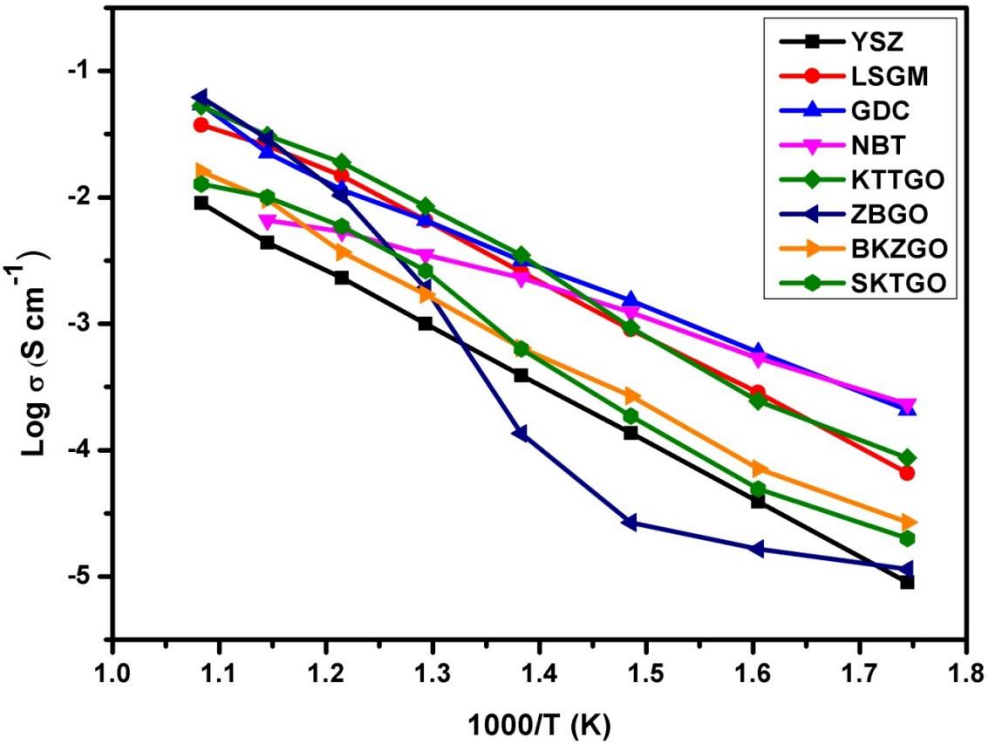

Fig 5.6 Comparison of ionic conductivities of existing intermediate Oxide-ion electrolytes in the air from Ref [5]

Figure 5.6 shows the Arrhenius plots of total electrical conductivity of $Sr_{1-x}K_xTi_{1-y}Ga_yO_{2-\delta}$ perovskite series with varying potassium and gallium concentration. The conductivity values are plotted against the 1000/T factor, and the slope is calculated by linearly fitting the curve using origin pro software. From the obtained slope, the activation energy is calculated using the following equation:

$$\sigma T = \sigma 0 \exp(\frac{-Ea}{kT}) \qquad \text{eq (5.3)}$$

Where σ_0 is the pre-exponential factor, E_a is the activation energy, k is the Boltzman constant, and T is the absolute temperature. The variation in total conductivity with respect to dopant concentration at various measured temperatures is depicted in figure 5.6. The activation energy for oxide-ion conductivity was as low as 0.52 eV for the $Sr_{0.8}K_{0.2}Ti_{0.8}Ga_{0.2}O_{2.8}$ sample. Thus it can be concluded that at temperatures ($T \geq 600^oC$), the ionic conductivity of the material is mainly due to oxide-ion vacancies.

5.7 Conclusion

It can be concluded that substitutions of K and Ga at Sr and Ti Sites, respectively, in $SrTiO_3$ lattice resulted in stoichiometric oxide-ion vacancy type point defect formation. The oxide-ion vacancy formation resulted in superior ionic conductivity above 600^oC in non-humidified atmospheres. It helped the material overcome the poor ionic conductivity problem at elevated temperatures ($T > 500^oC$), limiting the material's application as a conductive electrolyte for ceramic fuel cells. The oxide-ion conductivities obtained here for simultaneously K and Ga doped $SrTiO_3$ samples are superior or equivalent to the conductivity obtained for YSZ (yttria-stabilized zirconia) and other well-known ceramic oxide-ion electrolytes. The present study also opens the doors for the employment of novel structural design of materials to generate active oxide-ion vacancies and develop superior ionic conductors. The material can also be

explored in a high moisture-rich or humidified environment for its applications as a protonic conductor for ceramic fuel cells and hydrogen separating membrane formations.